JWPR
Journal of World's Poultry Research
2026, Scienceline Publication
J. World Poult. Res. 16(2): 224-241, 2026
Research Paper
DOI: https://dx.doi.org/10.36380/jwpr.2026.21
PII: S2322455X2600021-16
ISSN: 2322-455X

Molecular Characterization and Evaluation of Field Fowl Adenovirus Isolates in Specific Pathogen Free Chicken Embryonated Eggs

Sharifah Hanim Sy Ibrahim[1], Norfitriah Mohamed Sohaimi[1*], Mohd Hair Bejo[2], Abdul Rahman Omar[2], Mazlina Mazlan[2], Mohammad Afshar Farzad[1], and Ugwu Chidozie Clifford[2]

[1]*Department of Veterinary Laboratory Diagnosis, Faculty of Veterinary Medicine, University of Putra Malaysia, 43400 UPM Serdang, Selangor, Malaysia*
[2]*Department of Veterinary Pathology and Microbiology, Faculty of Veterinary Medicine, University of Putra Malaysia, 43400 UPM Serdang, Selangor, Malaysia*

*Corresponding author's E-mail: fitriahsohaimi@upm.edu.my

Received: March 28, 2026, Revised: April 29, 2026, Accepted: May 30, 2026, Published: June 30, 2026

ABSTRACT

Fowl adenoviruses (FAdVs) pose a substantial economic threat to global poultry production due to outbreaks of inclusion body hepatitis (IBH) and gizzard erosion. The present study aimed to characterize four Malaysian FAdV serotype 8b isolates (UPM2101, UPM2102, UPM2103, and UPM2401) through sequence analysis of the *hexon* and *fiber* genes to identify unique variations, while concurrently assessing viral infectivity via propagation in specific pathogen free (SPF) chicken embryonated eggs. The four FAdV field isolates were obtained from commercial broiler chickens in Malaysia presenting classical lesions. Isolates UPM2101, UPM2102, and UPM2103 were collected from farms in Johore in 2021, whereas UPM2401 was collected from Kedah in 2024. UPM2101, UPM2103, and UPM2401 originated from swollen, pale, and friable livers with petechial hemorrhages, whereas UPM2102 was isolated from a gizzard erosion case. Polymerase chain reaction (PCR) amplification confirmed the presence of FAdV in all samples. Sequence analysis revealed high nucleotide identity among the isolates. In the *hexon* gene, a nucleotide insertion at position 33 in UPM2101 and a substitution (C→T) at position 428 in UPM2401 resulted in non-synonymous amino acid changes. UPM2101 exhibited multiple amino acid substitutions at positions 225–234 with an additional glutamine at position 235, whereas UPM2401 showed a single substitution (A93T). In the *fiber* gene, nucleotide substitutions and a deletion were observed in the knob region, resulting in amino acid changes including S149T and R150A in UPM2103 and R150S in UPM2401. Phylogenetic analysis classified all isolates within serotype 8b, forming a closely related cluster. Propagation in embryonated eggs demonstrated efficient viral replication, with UPM2101 exhibiting earlier embryonic mortality than UPM2401, indicating potential differences in virulence. The findings of the current study indicated that the Malaysian FAdV serotype 8b field isolates are closely related yet exhibit distinct molecular variations that may influence viral replication efficiency and infectivity in embryonated eggs.

Keywords: *Fiber* gene, *Hexon* gene, Inclusion body hepatitis, Infectivity, Serotype 8b, Substitution, Virulence

INTRODUCTION

Fowl adenoviruses (FAdVs) are economically significant poultry pathogens worldwide, associated with clinical diseases in avian species, including inclusion body hepatitis (IBH), hepatitis-hydropericardium syndrome (HHS), and gizzard erosion (Hess, 2013; Islam et al., 2026). The FAdVs belong to the genus Aviadenovirus under the family *Adenoviridae* and are divided into five species (FAdV-A to FAdV-E) and 12 serotypes (Schachner et al., 2018). Fowl adenovirus is characterized as a non-enveloped virus with 70-90nm in diameter, surrounded by icosahedral capsids comprising double-stranded linear DNA genomes (Adel et al., 2021). Among the five recognized FAdV species (A-E), FAdV serotype 8b**, a** member of species E, is frequently associated with IBH outbreaks in broiler chickens, leading to significant economic losses in commercial poultry production (Schachner et al., 2018; Sohaimi et al., 2022). Affected

birds typically exhibit clinical signs such as weakness, depression, and inability to stand, with gross lesions including hepatomegaly, hepatic necrosis, and petechial haemorrhages (Mirzazadeh et al., 2020; Sadekuzzaman et al., 2024).

Molecular characterization of FAdVs is essential for understanding viral diversity, epidemiology, and pathogenic potential (Sabarudin et al., 2021). The *hexon* gene, which encodes the major capsid protein, contains antigenically important regions such as the L1 loop and is widely used for PCR-based detection and serotype classification (Meulemans et al., 2004; Shah et al., 2017; Niczyporuk, 2018). The *fiber* gene, particularly the knob domain, mediates viral attachment and host cell entry, and sequence variations in this region can influence tissue tropism and virulence (Hess, 2013; Schachner et al., 2016). Recent studies in Southeast Asia have highlighted the circulation of genetically diverse FAdV-8b strains in poultry flocks, emphasizing the need for continued surveillance and molecular investigation (Sohaimi et al., 2022; Pohuang et al., 2025).

Virus isolation and propagation in specific pathogen-free (SPF) embryonated chicken eggs remain critical for experimental characterization of FAdV isolates, enabling assessment of tissue tropism, pathogenicity, and the effect of genetic variations on viral replication (Alemnesh et al., 2012; Hess, 2013). Integrating molecular detection with experimental propagation provides a comprehensive approach to evaluating the biological behavior of field isolates and their epidemiological relevance.

Although FAdV serotype 8b has been reported in several Asian countries, there is limited information on the molecular characteristics, genetic variations, and pathogenic potential of recent field Malaysian isolates. In recent years, the number of reported IBH cases has continued to rise, even on commercial farms implementing local vaccination protocols. Such an increase may be attributed to genetic variations in key viral proteins among field isolates, potentially affecting vaccine efficacy and disease control (Sohaimi and Bejo, 2021). Consequently, these data limitations obstruct a comprehensive understanding of viral evolution, strain-specific virulence, and their potential impact on poultry health, complicating efforts to design effective surveillance and control strategies. The present study aimed to characterize recent Malaysian FAdV serotype 8b isolates by sequencing the *hexon* and *fiber* genes for unique variations, while utilizing specific pathogen free chicken embryonated eggs for viral propagation to assess infectivity and tissue tropism.

MATERIALS AND METHODS

Ethical approval

The study protocols described were undertaken in accordance with the criteria approved by the Institutional Animal Care and Use Committee (IACUC), University of Putra Malaysia, Selangor, Malaysia, under approval number UPM/IACUC/AUP-R056/2025.

Study designs

The present study was conducted to molecularly characterize recent field isolates of FAdV from Malaysia and to evaluate their propagation in specific pathogen free (SPF) chicken embryonated eggs. Field samples from suspected FAdV outbreaks were subjected to molecular detection, sequence analysis, and phylogenetic characterization targeting selected viral genes. Two positive isolates with distinct molecular variations were subsequently propagated in SPF embryonated chicken eggs to evaluate viral replication and associated embryonic lesions.

Sample origin

Suspected FAdV-positive samples (n = 4) were retrieved from the Virology Laboratory, Faculty of Veterinary Medicine, University of Putra Malaysia (UPM), Serdang, Selangor, Malaysia. The samples were associated with clinical signs and gross lesions suggestive of IBH, primarily involving the liver and gizzard. Samples of liver were collected from two commercial broiler chicken farms in Johore, Malaysia, in 2021 and from one commercial broiler chicken farm in Kedah, Malaysia, in 2024. A gizzard sample was also obtained from a commercial broiler chicken farm in Johore, Malaysia, in 2021.

A total of four isolates were obtained and designated as UPM2101, UPM2102, UPM2103, and UPM2401. The UPM2101 and UPM2102 were obtained from 23-day-old and 26-day-old broiler chickens, respectively, in a commercial farm in Johore from two different houses in 2021 with a history of 5% cumulative mortality rate. The UPM2103 isolate was obtained in 2021 from Johore from a 30-day-old commercial broiler chicken with a swollen and necrotic liver. The isolate UPM2401 was recovered from a liver sample collected directly from a 25-day-old broiler chicken in Kedah in 2024, where the flock showed a mortality rate of approximately 0.1% per week with 10% total mortality. Affected chickens from these farms exhibited clinical signs including weakness, depression, and inability to stand. Based on farm records, all poultry

flocks were vaccinated against Newcastle Disease Virus (NDV; Boehringer Ingelheim, Germany), infectious bursal disease virus (IBDV; Boehringer Ingelheim, Germany), infectious bronchitis (IB; Boehringer Ingelheim, Germany), and Marek`s Disease virus (MDV; Zoetis, USA).

Virus isolation

Sample collection and processing

Tissue samples (1.5 g of liver and gizzard) were collected and stored in -20°C prior to homogenization using a sterile mortar and pestle in phosphate-buffered saline (PBS) at a ratio of 1:10 (w/v) to prepare a 10% suspension, following previously published protocols for avian virus sample processing (Sadekuzzaman et al., 2024). The homogenized samples were treated with 1% antibiotic solution containing streptomycin (10 mg/mL; Biosera, France) and penicillin (10,000 IU/mL; Biosera, France), together with amphotericin B (25 µg/mL; Biosera, France) to minimize bacterial and fungal contamination. The mixture was then centrifuged at 1,509 × g for 10 minutes to clarify the supernatant. The clarified supernatant was subsequently passed through a 0.45 µm syringe filter to remove remaining cellular debris and potential microbial contaminants. Filtered suspensions were stored at -20°C until further analysis (Sadekuzzaman et al., 2024).

Molecular methods

DNA extraction and PCR amplification of the hexon and fiber genes

Viral genomic DNA was isolated from homogenized liver and gizzard tissues using a commercially available DNA extraction kit (Analytik Jena, Germany) in accordance with the manufacturer's protocol, which is based on a spin-column purification system. The purified DNA was then used as a template to amplify the hexon and fiber genes by conventional polymerase chain reaction (PCR). For the hexon gene, the previously published primer pair *HexonA1* and *HexonB1* was used as described by Sohaimi et al. (2022; Table 1).

Table 1. Primer set used for PCR amplification and sequence analysis of the *hexon* and fiber *genes* of fowl adenovirus

Target gene	Forward sequence (5` to 3`)	Reverse sequence (5` to 3`)	Amplicon size (bp)	Reference
Hexon	CAARTTCAGRCAGACGGT	TAGTGATGNCKSGACATCAT	897 bp	(Sohaimi et al., 2022)
Fiber	ACCGATTACGGCCGACGAAC	GAGCGTTGGCTGTGCTTAGG	940 bp	(Ugwu et al., 2020)

The *fiber* gene targeting the knob region was amplified using primers FbrF and FbrR, with an expected amplicon size of 940 bp (Ugwu et al., 2020; Table 1). For positive control, FAdV isolate UPM1901 was used in this study (Sohaimi et al., 2022). Sterile nuclease-free water was used as a negative control during PCR amplification. Amplification for both genes was performed in a total reaction volume of 50 µL using MyTaq™ Red Mix (Bioline, UK) according to the manufacturer's instructions. The amplification protocol consisted of 36 cycles of denaturation, annealing, and extension at 95°C for one minute, followed by annealing at 60°C for 1 minute using HexonA1/HexonB1 primers or 50°C for 1 minute using FbrF/FbrR primers, and extension at 72°C for 1.30 minutes. A final extension step was carried out at 72°C for 2 minutes. The amplified PCR products were separated by electrophoresis on a 1% agarose gel containing 6 µL of RedSafe™ Nucleic Acid Staining Solution (iNtRON, Korea) at 70 V for 45 minutes alongside a 1 kb DNA marker (GeneDireX™, Taiwan). The DNA bands were subsequently visualized under UV transillumination using a Bio-Rad Gel Doc system (USA).

Purification, sequencing, and nucleotide sequence analysis of PCR products

Four PCR-positive amplicons were purified using the iNtRON MEGAquick-spin™ Total Fragment DNA Purification Kit (iNtRON, Korea) and subsequently submitted for sequencing at 1st BASE (Singapore). The obtained nucleotide sequences were retrieved, assembled, and analysed using BioEdit Version 7.2.5 software as previously described by Sohaimi et al. (2022). Sequence verification was performed using the NCBI BLAST GenBank online database. Partial *hexon* (705 bp) and *fiber knob domain* (452 bp) gene sequences were obtained from four Malaysian FAdV isolates (UPM2101, UPM2102, UPM2103, and UPM2401) to assess nucleotide and amino acid variation. Nucleotide sequence comparisons among the FAdV isolates were performed through multiple sequence alignment (MSA) using the ClustalW program, while the percentage of sequence identity between isolates was determined using the sequence identity matrix function in BioEdit. The nucleotide sequences were further translated into amino acid sequences using the

ExPASy online translation tool and subsequently submitted to GenBank to obtain accession numbers. All *hexon* and *fiber* gene nucleotide sequences generated in the present study were deposited in GenBank under accession numbers PX984946–PX984949 (*hexon*) and PX984950–PX984953 (*fiber*).

Phylogenetic analysis

Phylogenetic tree construction

Thirty published FAdV *hexon* (Supplementary Table 1) and *fiber* (Supplementary Table 2) gene sequences were retrieved from the GenBank database. Duck adenovirus sequences under genus *Atadenovirus* were used as outgroups representing a different genus of avian adenovirus. Multiple nucleotide sequence alignments between recent FAdV isolates and 31 reference strains were performed using MEGA (version 12). Subsequently, the entire region of the L1 loop of *hexon* and *fiber* knob domain genes was used for phylogenetic tree analysis (Sohaimi et al., 2018). The p-distance model was used to compute the distance matrix and later utilized to infer phylogenetic construction through the Neighbour-joining method with 1000 bootstrap replicates (Juliana et al., 2014).

Propagation in eggs

Isolation and propagation of fowl adenovirus

Two FAdV isolates, UPM2101 and UPM2401, were selected for virus isolation and propagation in specific pathogen-free (SPF) embryonated chicken eggs. Both isolates were chosen based on the presence of notable molecular changes in the major capsid protein, particularly within the *hexon* gene, which constitutes a large portion of the viral surface and plays an important role in viral infectivity. Non-inoculated embryos were maintained throughout the experiment as negative controls. Virus propagation was performed using 9-day-old SPF embryonated chicken eggs. Briefly, 0.1 mL of the treated inoculum prepared from the original homogenate was inoculated into each egg via the chorioallantoic membrane (CAM) route under aseptic conditions following the method described by Alemnesh et al. (2012). Five eggs were assigned to each isolate during the first passage, followed by 10 eggs for each group in the second passage. For the third passage, twenty (20) embryos were used for each isolate to enhance viral propagation. A positive control using the FAdV isolate UPM1901 was also included in the present study. Following inoculation, the eggs were incubated at 37°C for 10 days post-inoculation (dpi) and monitored daily by candling to assess embryo viability. Endpoints such as embryo mortality, lesions on CAM, embryos (haemorrhage and stunting) and liver were recorded throughout the trial. All dead embryos were subjected to post-mortem examination to observe and record gross lesions on the liver and CAM. Subsequently, the liver and CAM tissues were collected and processed for detection of FAdV using conventional PCR and endpoint titration by 50% egg infectious dose EID_{50} (Reed and Muench, 1938).

Statistical analysis

Mutation frequencies were calculated as the proportion of mutated nucleotide sites relative to the total sequence length analyzed. Differences among isolates were evaluated using the Kruskal–Wallis test in IBM SPSS Statistics (version 25), with statistical significance set at a p-value less than 0.05 (Thompson et al., 1994). For embryonic time-to-mortality, the data were analyzed using survival analysis to compare the virulence of the two virus isolates. As 100% cumulative mortality was observed in all groups, virulence was assessed based on the rate of mortality (days post-inoculation until death) rather than mortality proportion. A Cox proportional hazards regression model was initially applied to evaluate the effects of isolate type and passage level on mortality across all serial passages (Passage 1, n : 5; Passage 2, n: 10; Passage 3, n: 20 per isolate). To further assess differences in virulence at the stage with the largest sample size, only passage 3 data were analyzed separately. Survival distributions were estimated using the Kaplan–Meier method, and differences between isolates were compared using the Log-Rank (Mantel–Cox) test. Median survival times were also determined for each isolate group. Statistical significance was set at a p-value less than 0.05. All analyses were performed using IBM SPSS Statistics (Hosmer et al., 2008; Cox et al., 2023).

RESULTS

Gross lesions

The liver from isolates UPM2101, UPM2103, and UPM2401 exhibited lesions associated with IBH caused by FAdV infection. The liver from UPM2101 was swollen, congested, and friable, with multiple petechial haemorrhages (Figure 1a), while UPM2103 showed a pale and enlarged liver with yellowish discoloration. In UPM2401, the liver was swollen and characterized by petechial haemorrhages with a multifocal area of necrosis (Figure 1b). Meanwhile, the gizzard from isolate UPM2102 exhibited typical gizzard erosion characterized

by erosion of the koilin layer, consistent with FAdV-associated adenoviral gizzard erosion (AGE).

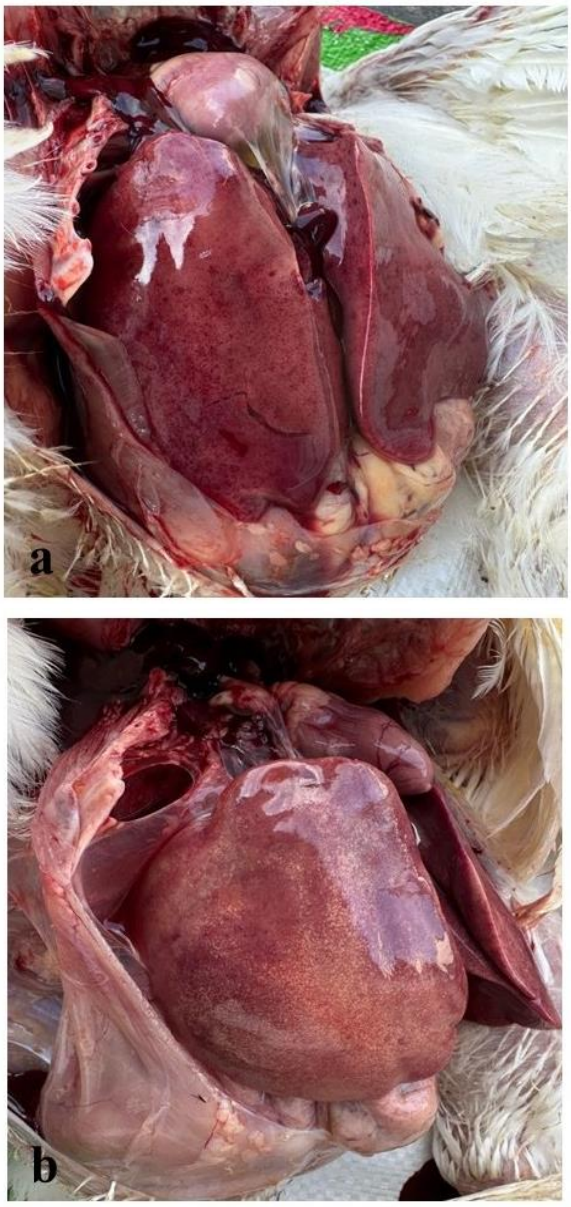

Figure 1. Gross hepatic lesions in commercial broiler chickens infected with fowl adenovirus isolates UPM2101 and UPM2401, obtained from 23-day-old and 25-day-old broiler chickens from farms in Johore (2021) and Kedah (2024), Malaysia, respectively. **a:** Swollen, congested, and friable liver with petechial haemorrhages (UPM2101 isolate). **b:** Swollen liver with petechial haemorrhages and multifocal areas of necrosis (UPM2401 isolate).

Molecular detection of fowl adenovirus

Samples UPM2101, UPM2103, and UPM2401 obtained from liver tissues and sample UPM2102 obtained from gizzard tissue tested positive for FAdV infection based on PCR amplification of the *hexon* (Figure 2a) and *fiber* genes (Figure 2b). Detection of both target genes therefore confirmed the presence and molecular characterization of the FAdV isolates.

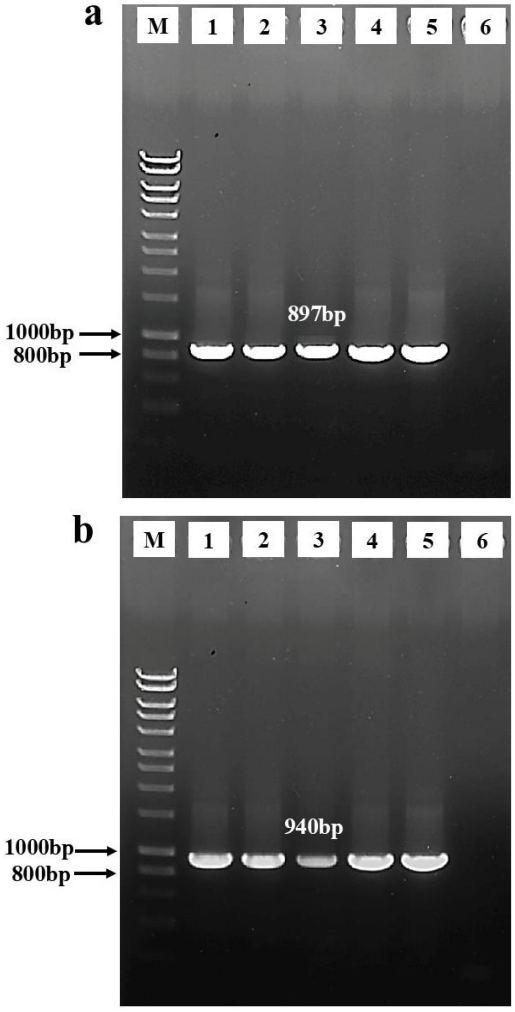

Figure 2. Electrophoresis of polymerase chain reaction products amplified using primers *HexonA1/HexonB1* and *FbrF/FbrR*. **a:** showing 897 base pairs (bp; *hexon*). **b:** 940 bp (*fiber*) amplicons of fowl adenovirus from four field isolates, namely UPM2101 (23-day-old), UPM2102 (26-day-old), UPM2103 (30-day-old), and UPM2401 (25-day-old) obtained from commercial broiler chickens in Johore (2021) and Kedah (2024), Malaysia, on a 1% agarose gel. Lane M: 1kb DNA marker, Lane 1: Positive control (UPM1901), Lane 2: UPM2101, Lane 3: UPM2102, Lane 4: UPM2103, Lane 5: UPM2401, Lane 6: Negative control.

Nucleotide and amino acid sequence analysis

BLAST analysis confirmed that all sequences corresponded to FAdV serotype 8b, showing high identity with reference strains in the GenBank database (E-value = 0.0).

Hexon gene

Pairwise nucleotide sequence analysis of the *hexon* gene demonstrated a high degree of similarity among the isolates, with nucleotide identities ranging from 99.7% to

100%. The identity was 100% between UPM2102 and UPM2103, whereas UPM2101 and UPM2401 exhibited slightly lower similarities of 99.7-99.8%, suggesting the presence of minor nucleotide variations within the L1 loop region of the *hexon* gene. In comparison with the Malaysian reference strain, UPM04217, all four field isolates shared 95% nucleotide identity in the *hexon* gene sequence. Multiple sequence alignment identified several nucleotide variations among the isolates, including a single nucleotide insertion (C) at position 33 in UPM2101 relative to the reference strain, UPM04217, and a substitution (C→T) at position 428 in UPM2401 compared with UPM2102 and UPM2103 isolates (Figure 3).

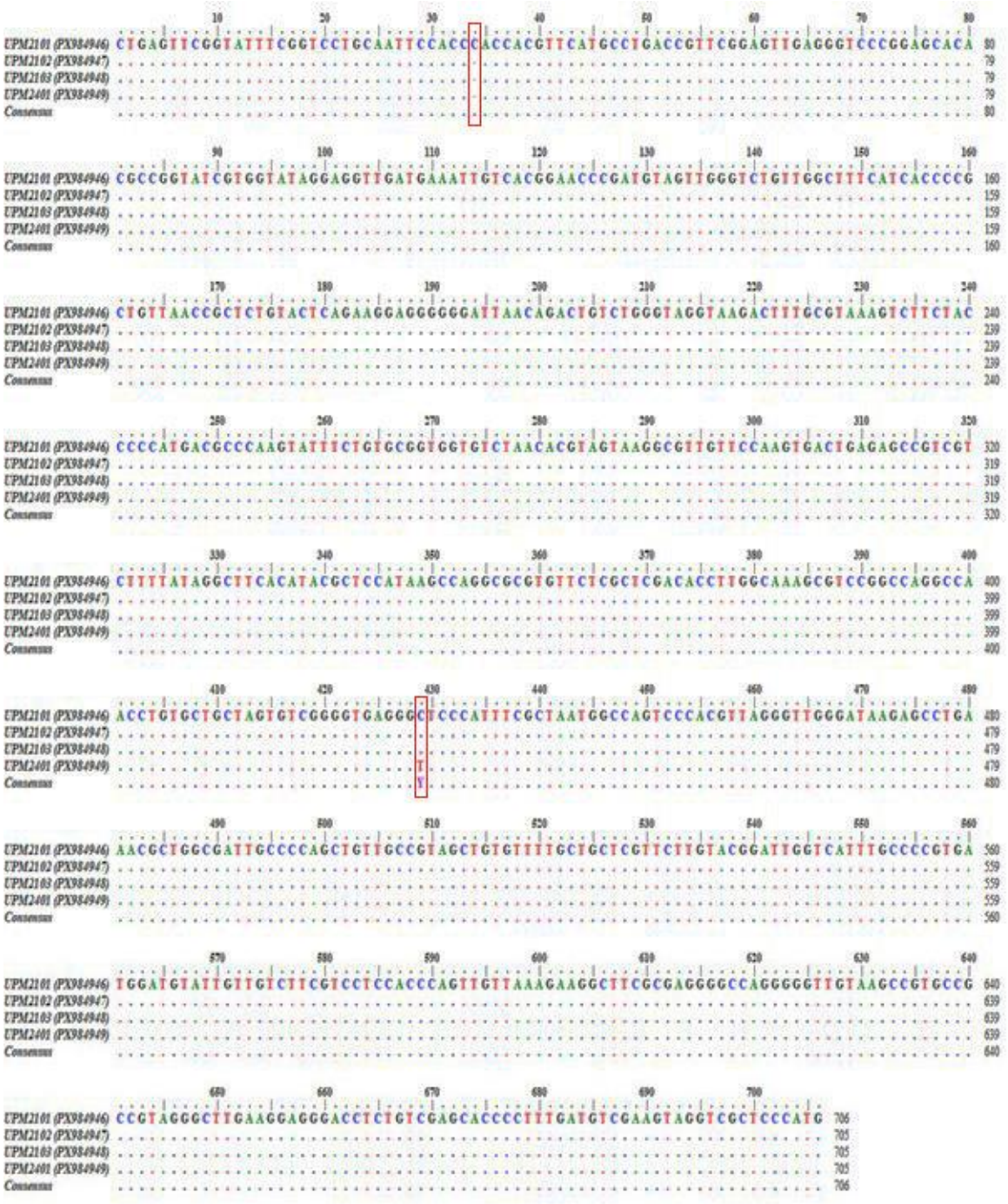

Figure 3. Multiple sequence alignment by ClustalW of 705 to 706bp nucleotide sequences of the L1 loop in the *hexon* gene between field fowl adenovirus isolates, UPM2101 (23-day-old), UPM2102 (26-day-old), and UPM2103 (30-day-old) obtained from commercial broiler chickens in Johore, Malaysia (2021), and UPM2401 (25-day-old) obtained from a commercial broiler chicken in Kedah, Malaysia (2024). Minor variations are indicated, including a single nucleotide insertion (C) at position 33 in UPM2101 and a C→T substitution at position 428 in UPM2401.

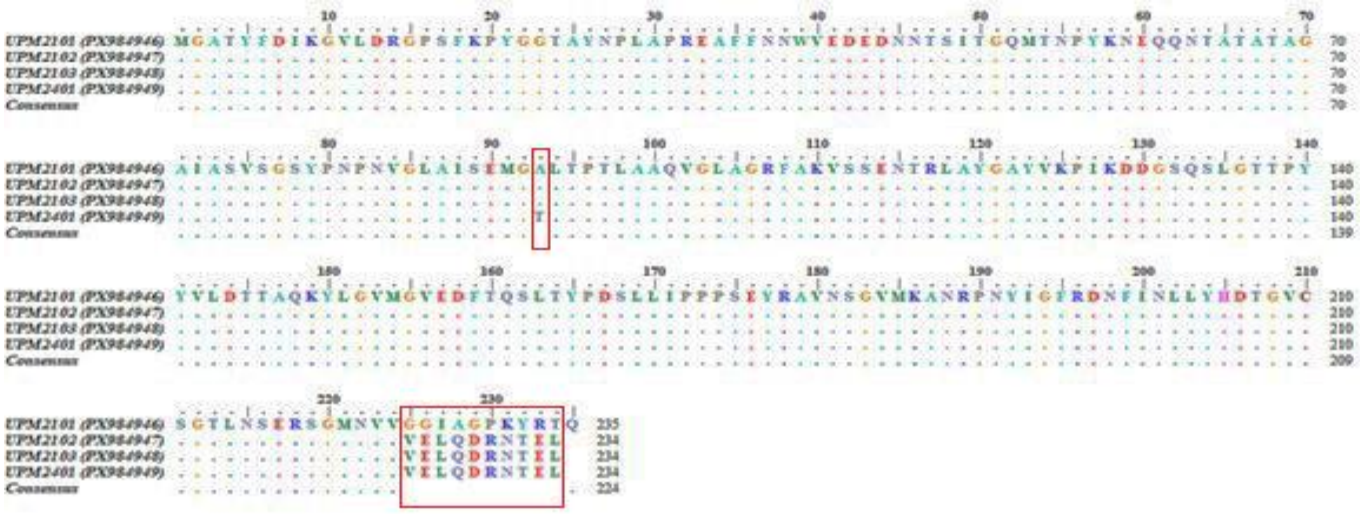

Figure 4. Multiple sequence alignment by ClustalW of 234 to 235 amino acid residues of the L1 loop in the *hexon* gene between recent field fowl adenovirus isolates, UPM2101 (23-day-old), UPM2102, (26-day-old), and UPM2103 (30-day-old) obtained from commercial broiler chickens in Johore, Malaysia (2021), and UPM2401 (25-day-old) obtained from a commercial broiler chicken in Kedah, Malaysia (2024). Amino acid variations are highlighted, including multiple substitutions covering residues 225-234 and an additional glutamine at position 235 in UPM2101 and a single substitution (A93T) in UPM2401.

Translation of the *hexon* gene sequences yielded 234-235 amino acids, with the observed nucleotide changes resulting in non-synonymous substitutions. A nucleotide insertion was identified in isolate UPM2101, leading to downstream amino acid alterations and the addition of an extra residue within the analyzed region. The insertion was consistently detected in both forward and reverse sequencing reads, suggesting that it was unlikely to be a sequencing artifact and likely represents a true biological variation, although its evolutionary origin remains to be determined. Notably, UPM2101 exhibited extensive amino acid alterations across residues 225-234, together with an additional glutamine at position 235 **(***G225V*, *G226E*, *I227L*, *A228Q*, *G229D*, *P230R*, *K231N*, *Y232T*, *R233E*, and *T234L)*. These changes occurred within the L1 loop of the *hexon* protein, a known hypervariable domain that contains key antigenic epitopes involved in immune recognition. In contrast, UPM2401 showed a single amino acid substitution (A93T), indicating a more conserved profile (Figure 4).

Fiber knob domain gene

Pairwise nucleotide sequence comparison of the *fiber* gene revealed high identity, ranging from 99.3% to 99.7%. The lowest identity (99.3%) was observed between UPM2101 and UPM2102/UPM2103, while the highest similarity (99.7%) was observed between UPM2401 and both UPM2102 and UPM2103, reflecting minor nucleotide differences among the isolates. In comparison with the Malaysian reference strain, UPM04217, all four field isolates shared 98% to 99% nucleotide identity in the *fiber* gene sequence.

Multiple sequence alignment of the *fiber* gene knob region identified several nucleotide substitutions and a deletion among the isolates (Figure 5). Several shared nucleotide substitutions were detected at positions 448 (C→A) and 451 (G→C) in UPM2102, UPM2103, and UPM2401 compared to UPM2101, indicating conserved evolutionary changes among these isolates. In addition, UPM2102, which originated from a gizzard erosion sample, exhibited a unique substitution at position 450 (C→A), while UPM2103, from a liver sample, showed a unique deletion at position 446.

Relative to UPM04217, UPM2101 carried a single substitution at position 448 (C→A), whereas UPM2401 shared substitutions at positions 448 (C→A) and 451 (G→C), suggesting a closer relatedness between UPM2101 and UPM2401 in the analyzed genomic region. At the amino acid level, the *fiber* gene encoded 150 residues, with non-synonymous substitutions detected in the knob domain. Specifically, UPM2103 showed S149T and R150A substitutions, while UPM2401 exhibited an R150S change (Figure 6). Despite the presence of minor nucleotide and amino acid variations, no significant differences in mutation frequencies were observed among the isolates in either the *hexon* or *fiber* genes ($p > 0.05$), consistent with the high sequence identities obtained.

Phylogenetic tree analysis

Phylogenetic analysis of 35 aligned nucleotide sequences from the partial *hexon* and *fiber* genes classified FAdVs into five species (A–E). The recent isolates UPM2101, UPM2102, UPM2103, and UPM2401 clustered within species E (serotype 8b), grouping closely with the Malaysian reference strain UPM04217 and the 764 strain in both the *hexon* (Figure 7) and *fiber* (Figure 8) gene trees.

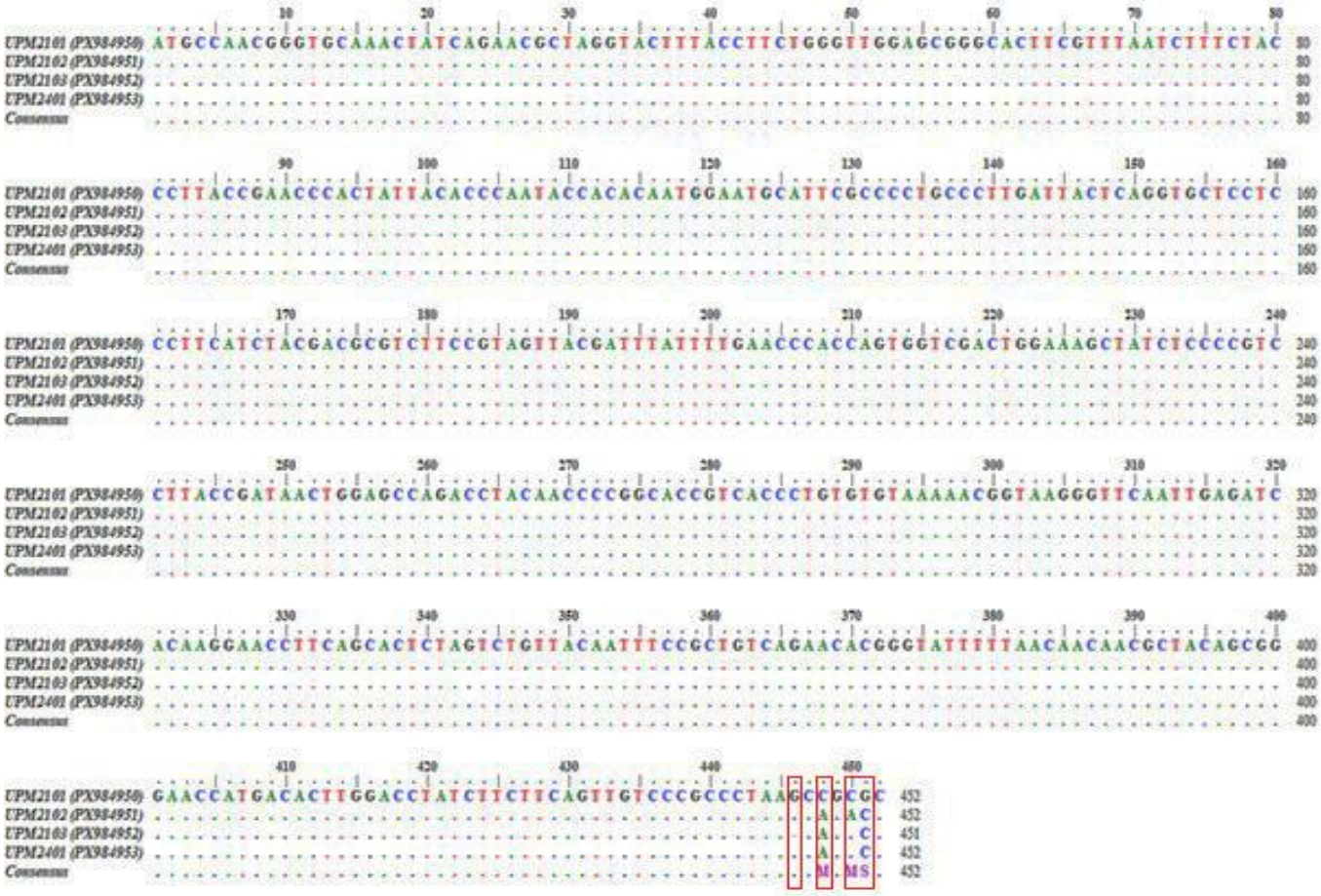

Figure 5. Multiple sequence alignment by ClustalW of 452bp nucleotide sequences of the knob region of the *fiber* gene of fowl adenovirus between field isolates, UPM2101 (23-day-old), UPM2102 (26-day-old), and UPM2103 (30-day-old) obtained from commercial broiler chickens in Johore, Malaysia (2021), and UPM2401 (25-day-old) obtained from a commercial broiler chicken in Kedah, Malaysia (2024). Several nucleotide changes were observed among the isolates including of UPM2102 (positions 448 C→A, 450 C→A, 451 G→C), UPM2103 (deletion at 446, 447 C→A, 450 G→C), and UPM2401 (448 C→A, 451 G→C).

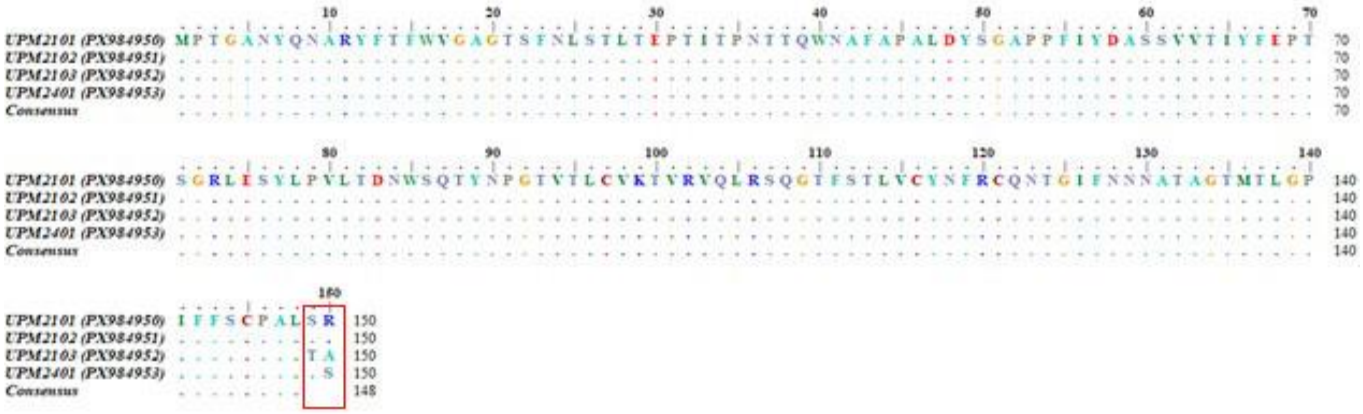

Figure 6. Multiple sequence alignment by ClustalW of 150 amino acid residues of the knob region in the *fiber* gene between recent fowl adenovirus isolates, UPM2101 (23-day-old), UPM2102 (26-day-old), and UPM2103 (30-day-old) obtained from commercial broiler chickens in Johore, Malaysia (2021), and UPM2401 (25-day-old) obtained from a commercial broiler chicken in Kedah, Malaysia (2024). Amino acid variations were identified within the *fiber* knob domain, including *S149T* and *R150A* in UPM2103 and R150S in UPM2401, compared with the remaining isolates.

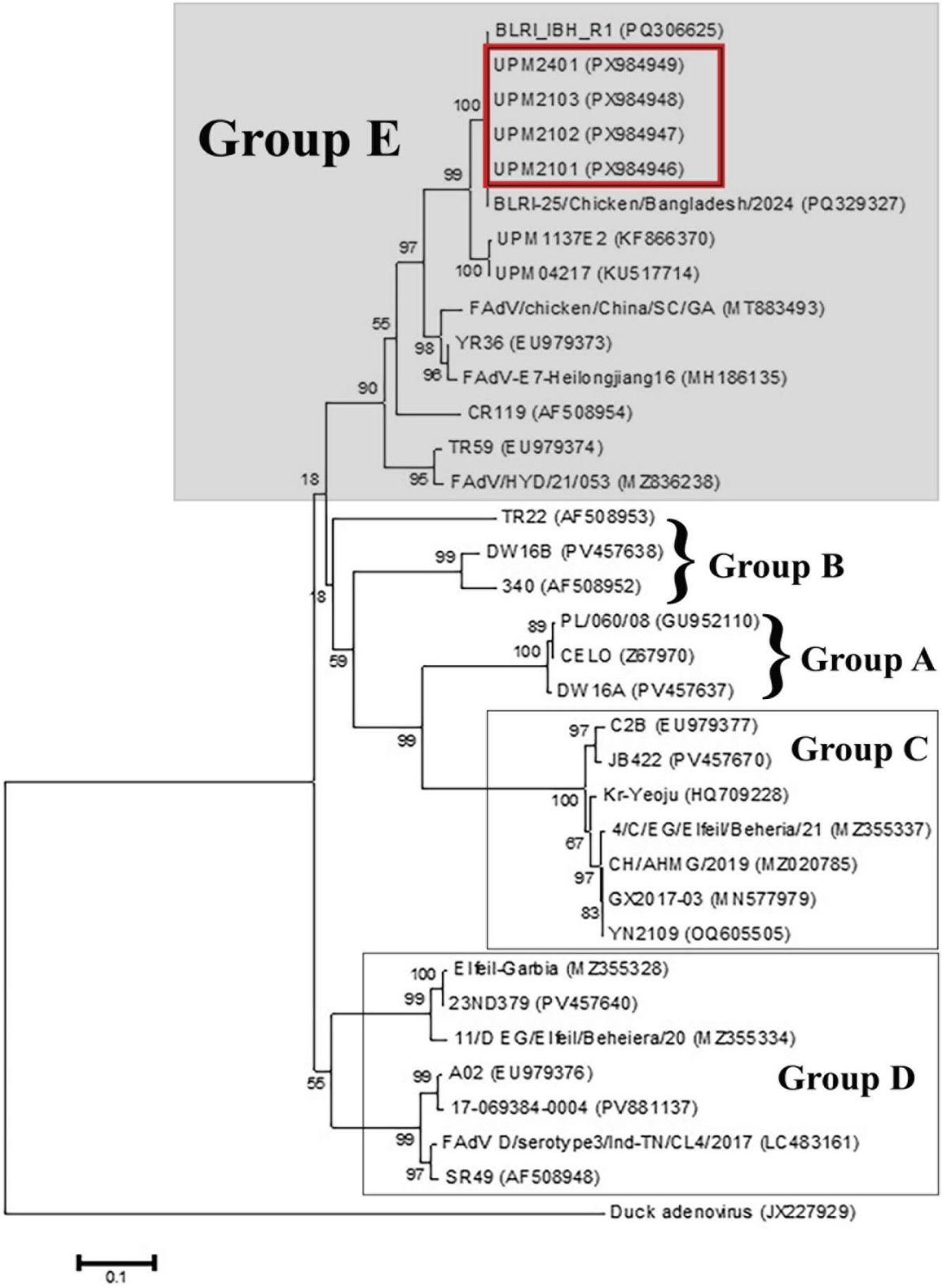

Figure 7. Phylogenetic analysis based on 706 nucleotides of the partial *hexon* gene of fowl adenovirus was performed, including the study isolates and 31 reference strains retrieved from the GenBank database. The isolates UPM2101, UPM2102, and UPM2103 obtained from commercial broiler chickens in Johore, Malaysia (2021) and UPM2401 obtained from a commercial broiler chicken in Kedah, Malaysia (2024) clustered within species E and were identified as FAdV serotype 8b.

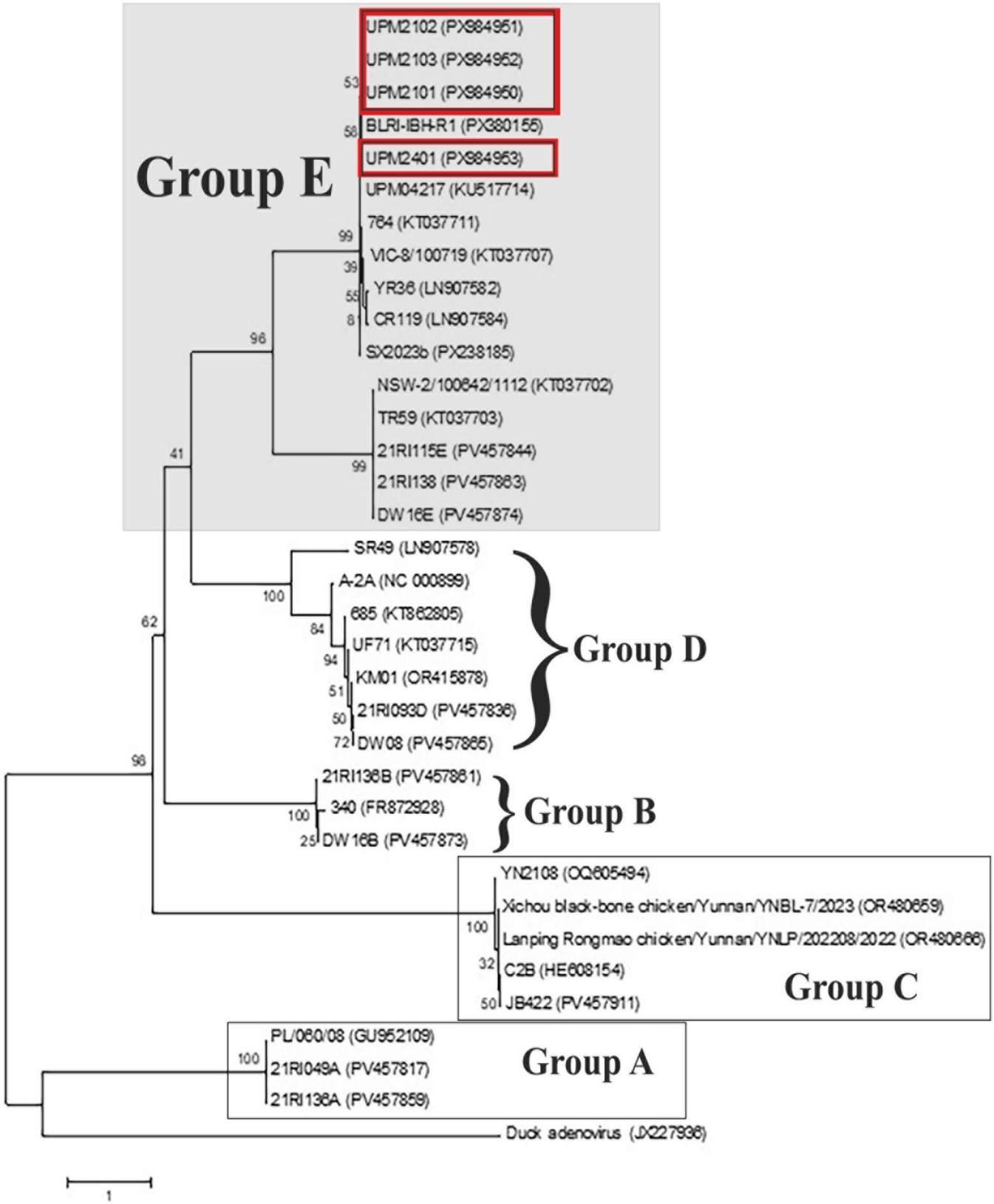

Figure 8. Phylogenetic analysis based on 452 nucleotides of the partial *fiber* gene of fowl adenovirus was performed, including the study isolates and 31 reference strains retrieved from the GenBank database. The isolates UPM2101, UPM2102, UPM2103, obtained from commercial broiler chickens in Johore, Malaysia (2021), and UPM2401, obtained from a commercial broiler chicken in Kedah, Malaysia (2024), clustered within species E and were identified as FAdV serotype 8b.

Isolation and propagation of fowl adenovirus

Embryonic mortality

Both isolates, UPM2101 and UPM2401, induced 100% embryonic mortality in SPF embryonated chicken eggs (CEE) across three serial passages (Figure 9). In the first passage (P1), early mortality observed at 1 day post-inoculation (dpi) was 40% for UPM2101 and 20% for UPM2401. Both isolates subsequently reached 100% mortality by 5 dpi.

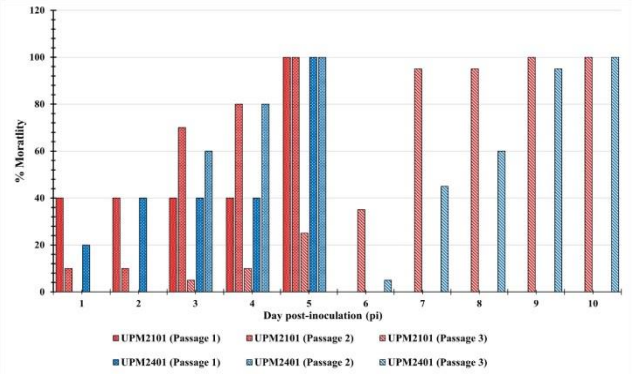

Figure 9. Cumulative embryo mortality (%) throughout three consecutive passages following inoculation with field fowl adenovirus isolates, UPM2101 and UPM2401, in SPF chicken embryonated eggs. Mortality was recorded daily, showing an earlier onset in UPM2101 than in UPM2401 and reaching 100% by the end of each passage.

In the second passage (P2), UPM2101 showed cumulative mortality of 10% at 2 dpi, 70% at 3 dpi, 80% at 4 dpi, and 100% at 5 dpi. UPM2401 exhibited 60% mortality at 3 dpi, 80% at 4 dpi, and 100% at 5 dpi, indicating comparable mortality kinetics among isolates under intermediate passage conditions. In the third passage (P3), marked differences in mortality patterns were observed between two isolates. The UPM2101 induced mortality started at 3 dpi and reached 100% by 9 dpi (5%, 10%, 25%, 35%, 95%, and 100% at 3 to 9 dpi, respectively). In comparison, UPM2401 showed a delayed onset at 6 dpi and reached 100% mortality by 10 dpi (5%, 45%, 60%, 95%, and 100% at 6 to 10 dpi, respectively). P3 data therefore demonstrated earlier onset and more rapid progression of embryonic mortality in UPM2101 compared with UPM2401.

Cox proportional hazards regression analysis across all passages (P1 to P3) did not show a significant overall difference in hazard rates between the two isolates ($p > 0.05$; Exp(B) = 0.625), likely due to variability in early passages where mortality patterns remained inconsistent. Therefore, comparative survival analysis was focused on passage 3 (n = 20 per isolate), which provided the most uniform and reliable data. Kaplan–Meier survival analysis of P3 demonstrated a significant difference in embryonic survival between isolates (Log-Rank $\chi^2 = 12.237$, df = 1, $P < 0.001$). UPM2101 exhibited a shorter median survival time (7 days) compared with UPM2401 (8 days), indicating a faster progression of embryonic mortality. These findings align with the P3 mortality kinetics, where UPM2101 showed earlier onset and more rapid accumulation of mortality. Consequently, virulence interpretation was based on survival kinetics (median survival time and hazard-based analysis), given that both isolates ultimately achieved 100% mortality across all passages.

Gross lesions, fowl adenovirus detection, and titration

Gross lesions in infected CEE were consistently observed in both UPM2101 and UPM2401 inoculated groups. Chorioallantoic membrane changes began as mild thickening at 2 to 4 days post-inoculation (dpi) and progressed to marked thickening and opacity from 5 dpi onwards (Figure 10a and 10b), indicating progressive viral replication and tissue involvement. The liver initially showed yellowish discoloration at 2 to 4 dpi, followed by multifocal necrosis, swelling, and petechial haemorrhages at 5 dpi onward (Figure 10c and 10d), reflecting progressive hepatic damage consistent with FAdV infection. Embryonic congestion was observed from 3 dpi in both isolates, further supporting systemic infection.

All liver samples tested positive for FAdV by PCR and remained consistently positive across all passages, confirming stable viral replication in chicken embryonated eggs. Virus titers reached $10^{6.8}EID_{50}$/mL for UPM2101 and $10^{6.6}EID_{50}$/mL for UPM2401 at passage 3.

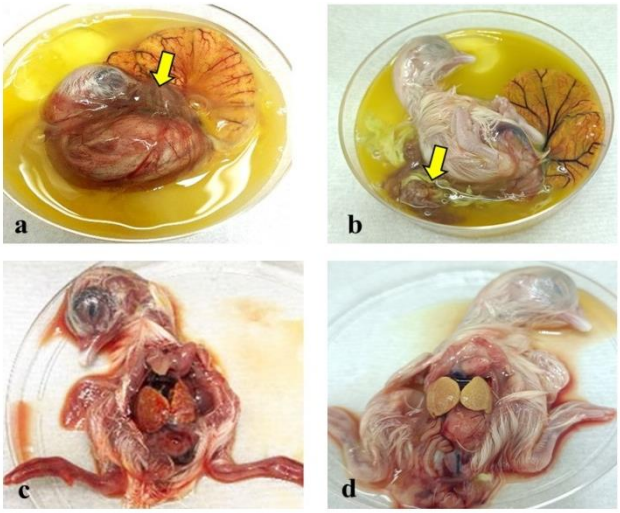

Figure 10. Gross lesions of infected embryos after inoculation with field fowl adenovirus isolates, UPM2101 and UPM2401, obtained from 23-day-old and 25-day-old broiler chickens from farms in Johore (2021) and Kedah (2024), Malaysia, respectively, at third passages. Thickening and cloudy chorioallantoic membrane (CAM) at **a**: 9 days post-inoculation (dpi) for UPM2101 and **b**: 10 dpi for UPM2401. **c**: Swollen, petechial haemorrhages with multifocal areas of necrosis in the liver at 9 dpi for UPM2101, **d**: Pale, multifocal areas of necrosis, and yellowish coloured liver in the embryo inoculated with UPM2401 at 10 dpi.

DISCUSSION

The present study characterized four Malaysian FAdV isolates (UPM2101, UPM2102, UPM2103, and UPM2401) based on gross lesions, molecular characteristics, phylogenetic relationships, and propagation in SPF CEE. The observed gross lesions were consistent with classical FAdV-induced pathology. Swollen, congested, and friable livers with petechial haemorrhages (UPM2101 and UPM2401), pale discoloration (UPM2103), and gizzard koilin erosion (UPM2102) align with previous reports of FAdV-associated IBH and gizzard erosion (Chitradevi et al., 2020; Shelke and Haque, 2025). Concurrent PCR detection of FAdV targeting the *hexon* and *fiber* genes further substantiates viral presence and supports the pathogenic potential of the isolates. Amplification of the *hexon* gene enabled molecular detection and serotype-related characterization of the isolates, while providing insights into viral antigenicity, tropism, and pathogenicity through its hypervariable regions. In addition, analysis of the *fiber* gene, which is involved in viral attachment and host-cell interactions, provided complementary molecular information on tissue tropism and virulence.

At the molecular level, the present findings demonstrated high overall similarity among the four Malaysian FAdV isolates, with sequence variation concentrated in the *hexon* and *fiber* genes. In the *hexon* gene, UPM2101 exhibited multiple non-synonymous substitutions at residues 225-235 of the L1 loop, a hypervariable region containing key antigenic epitopes. The substitution pattern suggests that UPM2101 may represent a more genetically divergent variant among the circulating strains, particularly within immunologically relevant regions. Such concentrated substitutions in the L1 loop may contribute to antigenic diversity and serotype differentiation while potentially altering host immune recognition and interactions, thereby influencing immune evasion, virulence, and pathogenicity. Overall, the findings indicate that UPM2101 possesses a higher degree of molecular variation with potential functional significance compared to the other isolates.

The present findings are supported by Mohamed and El-Sabagh (2022), who reported that amino acid variability within *hexon* loop 1 is closely associated with antigenic variation in FAdVs. Furthermore, Zhang et al. (2021) demonstrated that specific amino acid changes within the *hexon* protein can significantly influence viral pathogenicity, highlighting the functional importance of the *hexon* protein. Although the current study did not evaluate specific virulence-determining residues, such as R188 reported for FAdV-4 (Zhang et al., 2021), the accumulation of multiple substitutions within the same structural loop in UPM2101 suggests that comparable structural effects may contribute to differences in viral behaviour among circulating FAdV serotype 8b strains. In addition, a nucleotide insertion detected in UPM2101 resulted in downstream amino acid changes and length variation within the analysed region. Although the observed insertion variation was consistently observed in bidirectional sequencing reads, its biological validity remains inconclusive, as insertions may also arise from sequencing artefacts. Therefore, the functional significance of the identified mutation cannot be confirmed without further validation, and its potential impact on protein structure and viral phenotype remains speculative. Despite this limitation, its occurrence within an antigenically important region warrants further investigation. In contrast, UPM2401 exhibited only a single amino acid substitution, indicating a highly conserved profile among field isolates and suggesting limited variation within this lineage. The variation between the isolates further supports the presence of heterogeneity in evolutionary pressures acting on circulating strains (Sohaimi et al., 2022).

Similarly, *fiber* gene analysis in the present study revealed substitutions and a deletion within the knob domain, particularly in isolate UPM2103. The observed sequence variations indicate the presence of genetic variability among the Malaysian FAdV isolates. Given the role of the *fiber* knob domain in receptor recognition and host cell attachment, such variations may influence viral infectivity, tissue tropism, and host interactions (Zhang and Bergelson, 2005). Although the deletion identified in UPM2103 did not introduce a frameshift or premature stop codon, indicating preservation of the full-length *fiber* protein, it may cause localized structural alterations affecting protein conformation and viral attachment efficiency. Similar variability in the *fiber* knob and tail domains, including deletions, has been reported by Mohamed and El-Sabagh (2022), suggesting ongoing structural diversification within FAdVs. While sequence variation in the *fiber* gene has been documented among different FAdV serotypes, deletions within the knob region appear to be less common and may represent strain-specific molecular variation.

The potential functional significance of *fiber*-associated variation is supported by Yeo et al. (2023), who

demonstrated that genetic modifications in the *fiber* genes during serial passage can alter FAdV pathogenicity, with structural changes contributing to viral attenuation and vaccine-like phenotypes. Although the present isolates lacked frameshift mutations, the deletion and amino acid substitutions detected in UPM2103 may still affect viral biological properties. The potential biological significance of such genetic variation is supported by Qiao et al. (2024), who reported substantial genomic diversity among FAdV-8b strains (89.72-96.71% identity) and demonstrated that genetic variation can influence viral replication and pathogenicity *in vivo*. Overall, the findings suggest that genetic alterations within the *fiber* knob domain may contribute to functional variation among circulating FAdV-8b strains.

The phylogenetic clustering of the present isolates (UPM2101, UPM2102, UPM2103, and UPM2401) within FAdV species E, serotype 8b, and their close relationship to the previously reported Malaysian strain UPM04217 provide important epidemiological insights into FAdV circulation in the region. Such close genetic relatedness suggests a shared ancestral lineage and supports prolonged transmission of FAdV serotype 8b within Malaysian poultry populations rather than repeated introductions of genetically distinct strains (Sabarudin et al., 2021). The high sequence identity across both *hexon* and *fiber* genes further supports classification of these isolates within a closely related FAdV serotype 8b cluster, consistent with previous reports describing regional circulation of this serotype in Asia, such as Thailand, China, and Bangladesh (Chen et al., 2019; Sadekuzzaman et al., 2024; Pohuang et al., 2025).

From a regional perspective, clustering with earlier Malaysian isolates confirms that FAdV serotype 8b remains endemic in the local poultry industry and continues to be associated with IBH and adenoviral gizzard erosion (AGE; Sohaimi et al., 2022). It seems that continuous production cycles, frequent movement of personnel and materials, and subclinical infections likely perpetuate ongoing farm-to-farm spread and silent viral persistence (Sabarudin et al., 2021). Such conditions facilitate long-term circulation within integrated poultry networks, allowing the virus to remain established in the absence of major genetic variation processes. Thus, it will highlight the importance of continued molecular surveillance to monitor viral evolution and detect emerging variants with potential differences in tissue tropism or pathogenic behavior. Furthermore, the presence of unique nucleotide and amino acid variations within regions of the *hexon* and *fiber* proteins may contribute to differences in viral antigenic properties and could potentially influence disease outcomes among infected flocks (Qiao et al., 2024). Nevertheless, direct associations between specific mutations and observed gross lesion patterns cannot be established from the present data. The higher degree of amino acid variation in UPM2101 compared with other isolates suggests more pronounced molecular divergence, which may reflect differences in viral–host interactions at the protein level, whereas the more conserved profile of UPM2401 indicates variability in the extent of genetic change among circulating strains. In addition, findings from the current study, together with phylogenetic evidence, highlight the epidemiological significance of maintaining strict biosecurity measures and implementing targeted control strategies such as vaccination to minimize the impact of FAdV infection in poultry farms.

As compared to the previous Malaysian reports, earlier studies have primarily focused on detection and partial molecular characterization of FAdV strains, with a limited combination of pathological, phylogenetic, and comparative sequence analyses of both *hexon* and *fiber* genes in field isolates (Sohaimi et al., 2018). In contrast, the present study provides updated molecular characterization of recent Malaysian FAdV-8b isolates by combining pathological characterization, target-gene sequencing (*hexon* and *fiber*), and comparative analysis with earlier local reference strains. Notably, the detection of novel amino acid substitutions within the *hexon* L1 loop and the identification of a putative insertion in UPM2101, together with a deletion within the *fiber* knob region of UPM2103 and a conserved substitution profile in UPM2401, extend current knowledge of sequence-level variation in circulating strains. In addition, integration of molecular findings with phylogenetic clustering and gross lesion profiles provides a more comprehensive understanding of the current epidemiological status of FAdV-8b in Malaysia.

Isolation and propagation of selected isolates (UPM2101 and UPM2401) in SPF CEE were confirmed by their ability to induce 100% embryonic mortality across serial passages. Embryonic deaths occurring within the first 24 hours post-inoculation were considered non-specific, as non-comparable mortality was observed in the negative control group during the same period, indicating that they were likely associated with handling or inoculation-related stress rather than viral replication. Comparative survival analysis demonstrated that UPM2101 induced mortality earlier and exhibited a shorter median survival time (7 days) than UPM2401 (8

days), indicating a more rapid progression of embryonic death. At the molecular level, UPM2101 displayed greater genetic variability, including a unique nucleotide insertion and multiple amino acid substitutions within the *hexon* L1 loop, whereas UPM2401 exhibited only a single amino acid substitution in the *hexon* gene and an R150S substitution in the *fiber* gene. Although the present study did not directly assess the functional effects of the identified molecular alterations, the observed differences in mortality patterns may reflect variation in pathogenic characteristics between the two isolates. The progression of embryonic lesions, including CAM thickening, hepatic necrosis, and haemorrhages, further supports the pathogenic potential of the FAdV isolates and is consistent with characteristic FAdV infection (Alemnesh et al., 2012; Abghour et al., 2019; Safwat et al., 2022). In addition, consistent detection of FAdV in liver tissues across all passages confirms efficient viral replication and stability during propagation in embryonated eggs, demonstrating the value highlight the suitability of SPF CEE as a reliable model for virus isolation and pathogenicity assessment.

CONCLUSION

Malaysian FAdV isolates UPM2101, UPM2102, UPM2103, and UPM2401 caused classical FAdV-associated lesions and replicated efficiently in SPF embryonated eggs. High sequence identity classified all isolates as FAdV serotype 8b; however, minor genetic variations within the *hexon* and *fiber* genes suggest potential differences in virulence, antigenicity, and infectivity, as reflected by variations in embryonic mortality patterns. The findings expand current knowledge of circulating FAdV serotype 8b strains in Malaysia and underscore the importance of continuous molecular surveillance and the evolution of locally relevant vaccine strategies to enhance disease control in poultry populations. However, the present study was limited by the small number of isolates analyzed, partial gene sequencing, and the absence of *in vivo* challenge data. Future studies involving larger isolate collections, whole-genome sequencing, and experimental infection models are required to validate the present findings and further characterize the evolution and pathogenicity of FAdV serotype 8b.

DECLARATIONS

Authors' contributions

Norfitriah Mohamed Sohaimi and Mohd Hair Bejo conceptualized the study. Sharifah Hanim Sy Ibrahim, Mohammad Afshar Farzad, and Ugwu Chidozie Clifford developed the methodology. Sharifah Hanim Sy Ibrahim and Norfitriah Mohamed Sohaimi conducted the investigation, performed data curation, and carried out formal analysis. Sharifah Hanim Sy Ibrahim prepared the original draft of the manuscript. Norfitriah Mohamed Sohaimi, Mohd Hair Bejo, Mazlina Mazlan, and Abdul Rahman Omar reviewed and edited the manuscript. Norfitriah Mohamed Sohaimi, Mohd Hair Bejo, Mazlina Mazlan, and Abdul Rahman Omar supervised the study. Norfitriah Mohamed Sohaimi acquired the funding and administered the project. All authors read and approved the final manuscript before publication in the present journal.

Acknowledgements

The authors would like to express their gratitude to Mr. Saipuzaman Ali for invaluable assistance in the research activities.

Availability of the data and materials

The data obtained in this study are available upon reasonable request from the corresponding author.

Competing interests

The authors declared no competing interests.

Ethical considerations

Authors confirmed the originality of data, statistical analysis and the prepared article. During manuscript preparation, the authors utilized Gemini (an advanced language model developed by Google) for the sole purpose of language polishing, improving structural flow, and verifying academic nomenclature and formatting of the technical text. After using this tool, the authors thoroughly reviewed, verified, and edited the suggested content to ensure scientific accuracy and take full responsibility for the final integrity and factual correctness of the peer-reviewed text.

Funding

The present study was funded by the University of Putra Malaysia, Selangor, Malaysia, under the contract number GP-IPS (9806400).

REFERENCES

Abghour S, Zro K, Mouahid M, Tahiri F, Tarta M, Berrada J, and Kichou F (2019). Isolation and characterization of fowl aviadenovirus serotype 11 from chickens with inclusion body hepatitis in Morocco. PLoS One, 14(12): e0227004. DOI: https://www.doi.org/10.1371/journal.pone.0227004

Adel A, Mohamed AAE, Samir M, Hagag NM, Erfan A, Said M, Arafa AES, Hassan WMM, El Zowalaty ME, and Shahien MA (2021). Epidemiological and molecular analysis of circulating fowl adenoviruses and emerging of serotypes 1, 3, and 8b in Egypt. Heliyon, 7(12): e08366. DOI: https://www.doi.org/10.1016/j.heliyon.2021.e08366

Akopian TA, Doronin KK, Karpov VA, and Naroditsky BS (1996). Sequence of the avian adenovirus FAV 1 (CELO) DNA encoding

the hexon-associated protein pVI and hexon. Archives of Virology, 141(9): 1759-65. DOI: https://www.doi.org/10.1007/BF01718298

Alemnesh W, Hair-Bejo M, Aini I, and Omar AR (2012). Pathogenicity of fowl adenovirus in specific pathogen free chicken embryos. Journal of Comparative Pathology, 146(2-3): 223-229. DOI: https://www.doi.org/10.1016/j.jcpa.2011.05.001

Cha SY, Kang M, Park CK, Choi KS, and Jang HK (2013). Epidemiology of egg drop syndrome virus in ducks from South Korea. Poultry Science, 92(7): 1783-1789. DOI: https://www.doi.org/10.3382/ps.2013-03067

Chen W (2020). Fowl aviadenovirus 7 isolate FAdV/chicken/China/SC/GA hexon gene, partial cds. Genbank: MT883493. Available at: https://www.ncbi.nlm.nih.gov/nuccore/MT883493.1/

Chitradevi S, Sukumar K, Suresh P, Balasubramaniam GA, and Kannan D (2020). Molecular typing of fowl adenovirus associated with gizzard erosion in commercial layer grower chicken in Tamil Nadu. The Indian Journal of Animal Sciences, 90(7): 977-981. DOI: https://www.doi.org/10.56093/ijans.v90i7.106664

Chitradevi S, Sukumar K, Suresh P, Balasubramaniam GA, and Kannan D (2021). Molecular typing and pathogenicity assessment of fowl adenovirus associated with inclusion body hepatitis in chicken from India. Tropical Animal Health and Production, 53(4): 412. DOI: https://www.doi.org/10.1007/s11250-021-02851-8

Chen L, Yin L, Zhou Q, Peng P, Du Y, Liu L, Zhang Y, Xue C, and Cao Y (2019). Epidemiological investigation of fowl adenovirus infections in poultry in China during 2015-2018. BMC Veterinary Research, 15(1): 271. DOI: https://www.doi.org/10.1186/s12917-019-1969-7

Cox N, De Swaef E, Corteel M, Van Den Broeck W, Bossier P, Dantas-Lima JJ, and Nauwynck HJ (2023). The way of water: Unravelling white spot syndrome virus (WSSV) transmission dynamics in *Litopenaeus vannamei* shrimp. Viruses, 15(9): 1824. DOI: https://www.doi.org/10.3390/v15091824

Domanska-Blicharz K, Tomczyk G, Smietanka K, Kozaczynski W, and Minta Z (2011). Molecular characterization of fowl adenoviruses isolated from chickens with gizzard erosions. Poultry Science, 90(5): 983-9. DOI: https://www.doi.org/10.3382/ps.2010-01214

Elfeil WK and Abouelmaatti RR (2021a). Fowl aviadenovirus C isolate 4/C/EG/Elfeil/Beheria/21 hexon gene, partial cds. Genbank: MZ355337. Available at: https://www.ncbi.nlm.nih.gov/nuccore/MZ355337

Elfeil WK and Abouelmaatti RR (2021b). Fowl aviadenovirus D isolate 11/D EG/Elfeil/Beheiera/20 hexon gene, partial cds. Genbank: MZ355334. Available at: https://www.ncbi.nlm.nih.gov/nuccore/MZ355334

Elfeil WK (2021). Fowl aviadenovirus 2 isolate Elfeil-Garbia hexon gene, partial cds. Genbank: MZ355328. Available at: https://www.ncbi.nlm.nih.gov/nuccore/MZ355328

Hess M (2013). Avidenovirus infections. In: D. E. Swayne, J. R. Swayne, L. R. McDougald, L. K. Nolan, D. L. Suarez, and V. Nair (Editors), Diseases of poultry, 13th Edition. Blackwell Publishing Professional., Iowa, Ames, pp. 290-300. Available at: https://www.wiley.com/en-ag/Diseases+of+Poultry,+13th+Edition-p9781118719732

Hosmer DW, Lemeshow S, and May S (2008). Applied survival analysis: Regression modeling of time-to-event data. John Wiley & Sons, Inc., New Jersey, pp. 67-91. DOI: https://www.doi.org/10.1002/9780470258019.ch3

Isa NM, Mohd Ayob J, Ravi S, Mustapha NA, Ashari KS, Bejo MH, Omar AR, and Ideris A (2019). Complete genome sequence of fowl adenovirus-8b UPM04217 isolate associated with the inclusion body hepatitis disease in commercial broiler chickens in Malaysia reveals intermediate evolution. Virusdisease, 30(3): 426-432. DOI: https://www.doi.org/10.1007/s13337-019-00530-9

Islam MM, Nadia MMA, Islam MR, Islam MS, Sunny SA, Islam M, Sultana S, and Alam MJ (2026). Fowl adenovirus infections: A comprehensive review of prevalence, pathogenesis, diagnosis, control, and economic impact. Poultry Science, 105(4): 106565. DOI: https://www.doi.org/10.1016/j.psj.2026.106565

Juliana MA, Nurulfiza MI, Hair-Bejo M, Omar AR, and Aini I (2014). Molecular characterization of fowl adenoviruses isolated from inclusion body hepatitis outbreaks in commercial broiler chickens in Malaysia. Pertanika Journal of Tropical Agricultural Science, 37(4): 483-497. Available at: http://psasir.upm.edu.my/id/eprint/34573/

Karim MR, Samad MA, Uddin AA, Khan MMR, Akhter M, and Ali MZ (2024a). Fowl adenovirus 8b isolate BLRI_IBH_R1 hexon gene, partial cds. Genbank: PQ306625. Available at: https://www.ncbi.nlm.nih.gov/nuccore/PQ306625

Karim MR, Samad MA, Uddin AA, Khan MMR, Akhter M, and Ali MZ (2024b). Fowl adenovirus 8b strain BLRI-25/Chicken/Bangladesh/2024 hexon gene, partial cds. Genbank: PQ329327. Available at: https://www.ncbi.nlm.nih.gov/nuccore/PQ329327

Karim MR, Samad MA, Uddin AA, and Khan MMR (2025). Fowl adenovirus 8b isolate BLRI_IBH_R1, complete genome. Genbank: PX380155. Available at: https://www.ncbi.nlm.nih.gov/nuccore/PX380155

Lai J, Yang L, Chen F, He X, Zhang R, Zhao Y, Gao G, Mu W, Chen X, Luo S et al. (2023). Prevalence and molecular characteristics of FAdV-4 from indigenous chicken breeds in Yunnan province, Southwestern China. Microorganisms, 11(11): 2631. https://www.doi.org/10.3390/microorganisms11112631

Marek A, Nolte V, Schachner A, Berger E, Schlötterer C, and Hess M (2012). Two fiber genes of nearly equal lengths are a common and distinctive feature of fowl adenovirus C members. Veterinary Microbiology, 156(3-4): 411-417. DOI: https://www.doi.org/10.1016/j.vetmic.2011.11.003

Meulemans G, Couvreur B, Decaesstecker M, Boschmans M, and van den Berg TP (2004). Phylogenetic analysis of fowl adenoviruses. Avian Pathology, 33(2): 164-70. DOI: https://www.doi.org/10.1080/03079450310001652086

Mirzazadeh A, Asasi K, Mosleh N, Abbasnia M, and Abdi Hachesoo B (2020). A primary occurrence of inclusion body hepatitis in absence of predisposing agents in commercial broilers in Iran: A case report. Iranian Journal of Veterinary Research, 21(4): 314-318. DOI: https://www.doi.org/10.22099/ijvr.2020.36735.5360

Mohamed M and El-Sabagh I (2022). Molecular analysis of hexon and fiber genes of fowl aviadenoviruses isolated from field cases of inclusion body hepatitis. The Journal of Animal and Plant Sciences, 33(1): 191-200. DOI: https://www.doi.org/10.36899/japs.2023.1.0609

Niczyporuk JS (2018). Deep analysis of loop L1 HVRs1-4 region of the hexon gene of adenovirus field strains isolated in Poland. PLOS ONE, 13(11): e0207668. DOI: https://www.doi.org/10.1371/journal.pone.0207668

Niczyporuk JS, Kozdruń W, Czekaj H, Styś-Fijoł N, and Piekarska K (2020). Detection of fowl adenovirus D strains in wild birds in Poland by loop-mediated isothermal amplification (LAMP). BMC Veterinary Research, 16(1): 58. DOI: https://www.doi.org/10.1186/s12917-020-2271-4

Ojkic D, Lopes J, Sandrock C, Ratsep E, Brouwer E, Brooks A, Rossi T, and Martin E (2025). Fowl adenovirus 9 isolate 17-069384-0004 hexon gene, partial cds. Genbank: PV881137. Available at: https://www.ncbi.nlm.nih.gov/nuccore/PV881137

Ojkic D and Nagy E (2001). The long repeat region is dispensable for fowl adenovirus replication *in vitro*. Virology, 283(2): 197-206. DOI: https://www.doi.org/10.1006/viro.2000.0890

Park HS, Lim IS, Kim SK, Kim TK, and Yeo SG (2011). Isolation and characterization of fowl adenovirus serotype 4 from chickens with hydropericardium syndrome in Korea. Korean Journal of Veterinary Research, 51: 209-216. DOI: https://www.doi.org/10.14405/kjvr.2011.51.3.209

Pohuang T, Worawong K, Sarachu K, Khunbutsri D, and Junnu S (2025). Molecular characterization and phylogenetic diversity of fowl aviadenovirus serotype 8b associated with inclusion body hepatitis in Thai chickens. Veterinary World, 18(6): 1685-1693. DOI: https://www.doi.org/10.14202/vetworld.2025.1685-1693

Qiao Q, Yang P, Liu J, Xu M, Li Y, Li X, Xiang M, Zhu Y, Qiu L, Han C et al. (2024). Genome characterization of a novel fowl adenovirus serotype 8b isolate and construction of the reverse genetic system for rapid genome manipulation. Veterinary Microbiology, 298: 110262. DOI: https://www.doi.org/10.1016/j.vetmic.2024.110262

Rashid F, Xie Z, Zhang L, Luan Y, Luo S, Deng X, Xie L, Xie Z, and Fan Q (2020). Genetic characterization of fowl aviadenovirus 4 isolates from Guangxi, China, during 2017-2019. Poultry Science, 99(9): 4166-4173. DOI: https://www.doi.org/10.1016/j.psj.2020.06.003

Reed LJ and Muench H (1938). A simple method of estimating fifty per cent endpoints. American Journal of Epidemiology, 27(3): 493-497. DOI: https://www.doi.org/10.1093/oxfordjournals.aje.a118408

Sabarudin NS, Tan SW, Phang YF, and Omar AR (2021). Molecular characterization of Malaysian fowl adenovirus (FAdV) serotype 8b species E and pathogenicity of the virus in specific-pathogen-free chicken. Journal of Veterinary Science, 22(4): e42. DOI: https://www.doi.org/10.4142/jvs.2021.22.e42

Sadekuzzaman M, Miah MS, Parvin R, Haque ME, Islam TR, Sigma SH, Hossain MG, Hayat S, Hossain MT, and Islam MA (2024). Pathological investigation, molecular characterization and first-time isolation of the predominant serotypes of fowl adenovirus (FAdV-D and E) from commercial poultry in Bangladesh. Frontiers in Microbiology, 15: 1490255. DOI: https://www.doi.org/10.3389/fmicb.2024.1490255

Safwat MM, Sayed ASR, Ali Elsayed MF, and Ibrahim AAEH (2022). Genotyping and pathogenicity of fowl adenovirus isolated from broiler chickens in Egypt. BMC Veterinary Research, 18(1): 325. DOI: https://www.doi.org/10.1186/s12917-022-03422-1

Schachner A, Matos M, Grafl B, and Hess M (2018). Fowl adenovirus-induced diseases and strategies for their control - a review on the current global situation. Avian Pathology, 47(2): 111-126. DOI: https://www.doi.org/10.1080/03079457.2017.1385724

Schachner A, Marek A, Grafl B, and Hess M (2016). Detailed molecular analyses of the hexon loop-1 and fibers of fowl aviadenoviruses reveal new insights into the antigenic relationship and confirm that specific genotypes are involved in field outbreaks of inclusion body hepatitis. Veterinary Microbiology, 186: 13-20. DOI: https://www.doi.org/10.1016/j.vetmic.2016.02.008

Schachner A (2011). Fowl adenovirus B partial fiber gene, isolate 340. Genbank: FR872928. Available at: https://www.ncbi.nlm.nih.gov/nuccore/FR872928

Shah MA, Ullah R, March MD, Shah MS, Ismat F, Habib M, Iqbal M, Onesti S, and Rahman M (2017). Overexpression and characterization of the 100K protein of Fowl adenovirus-4 as an antiviral target. Virus Research, 238: 218-225. DOI: https://www.doi.org/10.1016/j.virusres.2017.06.024

Shankar KS, Priyanka E, Mathivanan B, Kumar Piruthiviraj B, Mukhopadhayay SK, Mondal Samiran, and Kannaki TR (2026). Molecular epidemiology of fowl adenovirus (FAdV) from inclusion body hepatitis (IBH) incidences from Indian broilers revealed the prevalence of serotypes of FAdV-D and E. Indian Journal of Animal Research, 60(5): 885-890. DOI: https://www.doi.org/10.18805/IJAR.B-4949

Shelke VM and Haque E (2025). Gizzard erosion in broilers: The fowl adenovirus (FAdV)-induced inclusion body hepatitis (IBH) poses a significant threat to the broiler. Agricultural Science Digest, 1: 1-10. DOI: https://www.doi.org/10.18805/ag.D-6278

Sohaimi NM, Clifford UC, and Hair-Bejo M (2022). Genetic diversity of fowl adenovirus serotype 8b isolated from cases of inclusion body hepatitis in commercial broiler chickens. Journal of the Indonesian Tropical Animal Agriculture, 47(2): 97-106. DOI: https://www.doi.org/10.14710/jitaa.47.2.97-106

Sohaimi NM, Bejo MH, Omar AR, Ideris A, and Isa NM (2018). Hexon and fiber gene changes in an attenuated fowl adenovirus isolate from Malaysia in embryonated chicken eggs and its infectivity in chickens. Journal of Veterinary Science, 19(6): 759-770. DOI: https://www.doi.org/10.4142/jvs.2018.19.6.759

Sohaimi NM and Hair-Bejo M (2021). A recent perspective on fiber and hexon genes proteins analyses of fowl adenovirus toward virus infectivity-A review. Open Veterinary Journal, 11(4): 569-580. DOI: https://www.doi.org/10.5455/OVJ.2021.v11.i4.6

Song H, Kim H, Kim J, Her M, and Kim H (2025). A novel species-specific multiplex PCR assay for the differentiation of five Fowl adenovirus species (A to E): Application to field surveillance. Poultry Science, 104(11): 105856. https://www.doi.org/10.1016/j.psj.2025.105856

Steer PA, Kirkpatrick NC, O'Rourke D, and Noormohammadi AH (2009). Classification of fowl adenovirus serotypes by use of high-resolution melting-curve analysis of the hexon gene region. Journal of Clinical Microbiology, 47(2): 311-321. DOI: https://www.doi.org/10.1128/JCM.01567-08

Steer PA, Agnew-Crumpton R, Scott PC, Browning GF, and Noormohammadi AH (2015a). Fowl aviadenovirus 11 isolate UF71 fiber gene, complete cds. Genbank: KT037715. Available at: https://www.ncbi.nlm.nih.gov/nuccore/KT037715

Steer PA, Agnew-Crumpton R, Scott PC, Browning GF, and Noormohammadi AH (2015b). Fowl adenovirus 8a isolate TR59 fiber gene, complete cds. Genbank: KT037703. Available at: https://www.ncbi.nlm.nih.gov/nuccore/KT037703

Steer PA, Agnew-Crumpton R, Scott PC, Browning GF, and Noormohammadi AH (2015c). Fowl adenovirus 8a isolate NSW-2/100642/1112 fiber gene, complete cds. Genbank: KT037702. Available at: https://www.ncbi.nlm.nih.gov/nuccore/KT037702

Steer PA and Noormohammadi AH (2015a). Fowl adenovirus 8b isolate 764 fiber gene, complete cds. Genbank: KT037711. Available at: https://www.ncbi.nlm.nih.gov/nuccore/KT037711

Steer PA and Noormohammadi AH (2015b). Fowl adenovirus 8b isolate VIC-8/100719 fiber gene, complete cds. Genbank: KT037707. Available at: https://www.ncbi.nlm.nih.gov/nuccore/KT037707

Su Q (2018). Fowl aviadenovirus 7 strain FAdV-E7-Heilongjiang16 hexon gene, partial cds. Genbank: MH186135. Available at: https://www.ncbi.nlm.nih.gov/nuccore/MH186135

Thompson JD, Higgins DG, and Gibson TJ (1994). CLUSTAL W: Improving the sensitivity of progressive multiple sequence alignment through sequence weighting, position-specific gap penalties and weight matrix choice. Nucleic Acids Research, 22(22): 4673-4680. DOI: https://www.doi.org/10.1093/nar/22.22.4673

Ugwu CC, Hair-Bejo M, Nurulfiza MI, Omar AR, and Ideris A (2020). Propagation and molecular characterization of fowl adenovirus serotype 8b isolates in chicken embryo liver cells adapted on Cytodex™ 1 microcarrier using stirred tank bioreactor. Processes, 8(9): 1065. DOI: https://www.doi.org/10.3390/pr8091065

Xue X, Zhang Z, Yang Q, Wang W, and Song J (2025). Epidemiological investigation and fiber gene genetic analysis of fowl adenovirus serotype 4 from 2017 to 2021 in Yunnan Province, China. Journal of Veterinary Science, 26(3): e27. DOI: https://www.doi.org/10.4142/jvs.24121

Yeo JI, Lee R, Kim H, Ahn S, Park J, and Sung HW (2023). Genetic modification regulates pathogenicity of a fowl adenovirus 4 strain after cell line adaptation (genetic mutation in FAdV-4 lowered pathogenicity). Heliyon, 9(9): e19860. DOI: https://www.doi.org/10.1016/j.heliyon.2023.e19860

Zhang Y, Liu A, Wang Y, Cui H, Gao Y, Qi X, Liu C, Zhang Y, Li K, Gao L et al. (2021). A single amino acid at residue 188 of the hexon protein is responsible for the pathogenicity of the emerging novel virus fowl adenovirus 4. Journal of Virology, 95(17): e0060321. DOI: https://www.doi.org/10.1128/JVI.00603-21

Zhang Y and Bergelson JM (2005). Adenovirus receptors. Journal of Virology, 79(19): 12125-12131. DOI: https://www.doi.org/10.1128/jvi.79.19.12125-12131.2005

Zhang J, Xie Z, Pan Y, Chen Z, Huang Y, Li L, Dong J, Xiang Y, Zhai Q, Li X et al. (2024). Prevalence, genomic characteristics, and pathogenicity of fowl adenovirus 2 in Southern China. Poultry Science, 103(1): 103177. DOI: https://www.doi.org/103177.10.1016/j.psj.2023.103177

Zhao L, Zhang X, and Zhang L (2021). Fowl adenovirus isolate CH/AHMG/2019, complete genome. Genbank: MZ020785. Available at: https://www.ncbi.nlm.nih.gov/nuccore/MZ020785

Supplementary Table 1. Fowl adenoviruses reference strains retrieved from the GenBank database for the *hexon* gene phylogenetic tree construction

No	FAdV Strain	Species	Serotype	Accession Number	Uploaded by
1	CELO	A	1	Z67970	Akopian et al. (1996)
2	PL/060/08	A	1	GU952110	Domanska-Blicharz et al. (2011)
3	DW16A	A	1	PV457637	Song et al. (2025)
4	340	B	5	AF508952	Meulemans et al. (2004)
5	TR22	B	5	AF508953	Meulemans et al. (2004)
6	DW16B	B	5	PV457638	Song et al. (2025)
7	Kr-Yeoju	C	4	HQ709228	Park et al. (2011)
8	4/C/EG/Elfeil/Beheria/21	C	4	MZ355337	Elfeil and Abouelmaatti (2021a)
9	CH/AHMG/2019	C	4	MZ020785	Zhao et al. (2021)
10	GX2017-03	C	4	MN577979	Rashid et al. (2020)
11	YN2109	C	4	OQ605505	Xue et al. (2025)
12	C2B	C	10	EU979377	Steer et al. (2009)
13	JB422	C	10	PV457670	Song et al. (2025)
14	Elfeil-Garbia	D	2	MZ355328	Elfeil (2021)
15	23ND379	D	2	PV457640	Song et al. (2025)
16	FAdV D/serotype3/Ind-TN/CL4/2017	D	3	LC483161	Chitradevi et al. (2021)
17	SR49	D	3	AF508948	Meulemans et al. (2004)
18	A02	D	9	EU979376	Steer et al. (2009)
19	17-069384-0004	D	9	PV881137	Ojkic et al. (2025)
20	11/D EG/Elfeil/Beheiera/20	D	11	MZ355334	Elfeil and Abouelmaatti (2021b)
21	CR119	E	6	AF508954	Meulemans et al. (2004)
22	YR36	E	7	AF508955	Meulemans et al. (2004)
23	FAdV-E7-Heilongjiang16	E	7	MH186135	Su (2018)
24	FAdV/chicken/China/SC/GA	E	7	MT883493	Chen (2020)
25	TR59	E	8a	EU979374	Steer et al. (2009)
26	FAdV/HYD/21/053	E	8a	MZ836238	Shankar et al. (2026)
27	BLRI_IBH_R1	E	8b	PQ306625	Karim et al. (2024a)
28	BLRI-25/Chicken/Bangladesh/2024	E	8b	PQ329327	Karim et al. (2024b)
29	UPM04217	E	8b	KU517714	Isa et al. (2019)
30	UPM1137E2	E	8b	KF866370	Sohaimi et al. (2018)
31	Duck adenovirus	NA	N/A	JX227929	Cha et al. (2013)

N/A: Not applicable (belongs to *the Adenovirus* genus)

Supplementary Table 2. Fowl adenoviruses reference strains retrieved from the GenBank database for *fiber* gene phylogenetic tree construction

No	FAdV Strain	Species	Serotype	Accession Number	Uploaded by
1	PL/060/08	A	1	GU952110	Domanska-Blicharz et al. (2011)
2	21RI136A	A	1	PV457859	Song et al. (2025)
3	21RI049A	A	1	PV457817	Song et al. (2025)
4	340	B	5	FR872928	Schachner (2011)
5	DW16B	B	5	PV457873	Song et al. (2025)
6	21RI136B	B	5	PV457861	Song et al. (2025)
7	YN2108	C	4	OQ605494	Xue et al. (2025)
8	Xichou black-bone chicken/Yunnan/YNBL-7/2023	C	4	OR480659	Lai et al. (2023)
9	Lanping Rongmao chicken/Yunnan/YNLP/202208/2022	C	4	OR480666	Lai et al. (2023)
10	C2B	C	10	HE608154	Marek (2012)
11	JB422	C	10	PV457911	Song et al. (2025)
12	685	D	2	KT862805	Niczyporuk et al. (2020)
13	KM01	D	2	OR415878	Zhang et al. (2024)
14	SR49	D	3	LN907578	Schachner (2016)
15	A-2A	D	9	NC_000899	Ojkic and Nagy (2001)
16	UF71	D	11	KT037715	Steer et al. (2015a)
17	DW08	D	11	PV457865	Song et al. (2025)
18	21RI093D	D	11	PV457836	Song et al. (2025)
19	CR119	E	6	LN907584	Schachner (2016)
20	YR36	E	7	LN907582	Schachner (2016)
21	TR59	E	8a	KT037703	Steer et al. (2015b)
22	NSW-2/100642/1112	E	8a	KT037702	Steer et al. (2015c)
23	DW16E	E	8a	PV457874	Song et al. (2025)
24	764	E	8b	KT037711	Steer and Noormohammadi (2015 a,b)
25	VIC-8/100719	E	8b	KT037707	Steer and Noormohammadi (2015 a,b)
26	UPM04217	E	8b	KU517714	Isa et al. (2019)
27	SX2023b	E	8b	PX238185	Wu (2025)
28	BLRI_IBH_R1	E	8b	PX380155	Karim et al. (2025)
29	21RI115E	E	8b	PV457844	Song et al. (2025)
30	21RI138	E	8b	PV457863	Song et al. (2025)
31	Duck adenovirus	NA	N/A	JX227936	Cha et al. (2013)

N/A: Not applicable (belongs to *the Adenovirus* genus), FAdV: Fowl adenoviruses